Journal of Alloys and Compounds 504S (2010) S22–S26

Contents lists available at ScienceDirect

Journal of Alloys and Compounds

journal homepage: www.elsevier.com/locate/jallcom

Preparation of $(Ti_{0.45}Cu_{0.378}Zr_{0.10}Ni_{0.072})_{100-x}Sn_x$ bulk metallic glasses

K.F. Xie [a,b], K.F. Yao [a,*], T.Y. Huang [a]

[a] Key Laboratory for Advanced Materials Processing Technology, Ministry of Education, Department of Mechanical Engineering, Tsinghua University, Beijing 100084, China
[b] Department of Mechanical Engineering, Nanchang Institute of Technology, Nanchang, Jiangxi 330099, China

ARTICLE INFO

Article history:
Received 4 July 2009
Received in revised form 16 February 2010
Accepted 27 February 2010
Available online 7 March 2010

Keywords:
Bulk metallic glasses
Ti-based alloy
Glass-forming ability
Mechanical properties

ABSTRACT

The quinary alloys of Ti–Cu–Zr–Ni–Sn, $(Ti_{0.45}Cu_{0.378}Zr_{0.10}Ni_{0.072})_{100-x}Sn_x$ (x = 0, 2, 4, 6, and 8 at.%), have been prepared and studied. The $(Ti_{0.45}Cu_{0.378}Zr_{0.10}Ni_{0.072})_{100-x}Sn_x$ (x = 0, 2, 4, 6) bulk glassy rods can been prepared by copper-mold casting. Among these glassy alloys, the $(Ti_{0.45}Cu_{0.378}Zr_{0.10}Ni_{0.072})_{98}Sn_2$ shows better glass-forming ability than others. Thermal analysis results show that the supercooled liquid range of the Ti–Cu–Zr–Ni glassy alloy has been increased with the addition of Sn. In addition, the as-prepared $(Ti_{0.45}Cu_{0.378}Zr_{0.10}Ni_{0.072})_{98}Sn_2$ glassy alloy exhibits yield strength and fracture strength of 2260 and 2650 MPa, respectively, together with a compressive plastic strain of 7.6%. The results show that the quinary Ti–Cu–Zr–Ni–Sn bulk glassy alloy possesses good mechanical properties.

1. Introduction

Bulk metallic glasses (BMGs) have been attracted more and more attention of scientists and engineers since they behave many excellent properties, such as unique magnetic, mechanical, electrical and anti-corrosion properties [1]. As one of the families of amorphous alloys, Ti-based bulk metallic glasses possess not only good mechanical properties but also low density and high specific strength [2,3]. Hence, they are more attractive than other BMGs when used as structural materials, which stimulates scientists to develop Ti-based BMGs. Up to date, much progress in the development of Ti-based BMGs alloys has been obtained [4–8]. Such as the typical Ti-based BMG, so-called Vit-Light alloy of $Ti_{45}Zr_{20}Be_{35}$, possesses a critical size of ~6 mm and a fracture strength of ~1860 MPa, a total strain of ~2.2% (mainly elastic), a density of ~4.59 g cm^{-3}, and a specific strength of ~405 J g^{-1} [9]. Another typical bulk glassy alloy is $Ti_{40}Zr_{10}Cu_{34}Pd_{14}Sn_2$, which possesses a critical size about 10 mm and a fracture strength of ~2050 MPa, a supercooled liquid range of ~50 K [10,11]. In addition, some other Ti-based BMGs have also been developed in Ti–Cu–Ni and Ti–Zr–Ni alloy systems [12–14]. However, if comparing with other BMG systems, such as Zr- or Pd-based BMGs, the glass-forming ability (GFA) of Ti-based BMGs is still relatively low, especially for those without containing Be or Pd elements. Then, enhancing the glass-forming ability of Ti-based BMGs is important and necessary.

Possessing high strength is an important and attractive character of BMGs despite that most of them show very limited global plasticity [15]. It is known that Ti-based BMGs usually exhibit higher strength than Zr- or Pd-based BMGs [16]. If the strength and even the plasticity of the Ti-based BMGs could be improved, it would be of great meaning. According to some reported results, it is known that suitable addition of some elements into an alloy is an effective way to enhance the glass-forming ability and improve the mechanical properties [1,2,17]. In this paper, the element Sn is served as the minor addition into a quaternary alloy of Ti–Cu–Zr–Ni. The GFA and the mechanical properties of the designed and prepared Ti–Cu–Zr–Ni–Sn alloys have been studied.

2. Experimental details

Ingots of Ti–Cu–Zr–Ni–Sn alloys in the nominal compositions of $(Ti_{0.45}Cu_{0.378}Zr_{0.10}Ni_{0.072})_{100-x}Sn_x$ (x = 0, 2, 4, 6 and 8 at.%) were prepared by melting pure elements (99.99 wt.% purity for Ti, Cu, Zr, Ni and Sn elements) under Ti-getter purified argon atmosphere with voltaic arc (see Fig. 1(a)). The button-shaped ingots were re-melted and turned at least 4 times for homogeneity, and then cast into a copper-mold with cylindrical cavity of certain diameter to produce a rod of round cross-section (see Fig. 1(b)). The as-cast alloy rods were examined by X-ray diffraction (XRD) with monochromatic *Cu Ka* radiation. The glassy structure was also confirmed by transmission electron microscopy (TEM) operating at 200 kV. The thin foil specimens for TEM observation were prepared by a standard twin-jet electrochemical polishing with a solution of 23% $HClO_4$ and 77% CH_3COOH at −30 °C. The thermal stability of the samples was examined by differential scanning calorimetry (DSC) at a heating rate of 0.33 K s^{-1}. The compression tests are conducted by using a DSS-25T machine at a strain rate of 4×10^{-4} s^{-1}. The compression test samples are prepared with dimension of 1 mm in diameter and 2 mm in length. The fracture surface and side views of the deformed samples were examined by scanning electron microscopy (SEM).

* Corresponding author. Tel.: +86 10 62772292; fax: +86 10 62772292.
E-mail address: kfyao@tsinghua.edu.cn (K.F. Yao).

0925-8388/$ – see front matter © 2010 Elsevier B.V. All rights reserved.
doi:10.1016/j.jallcom.2010.02.199

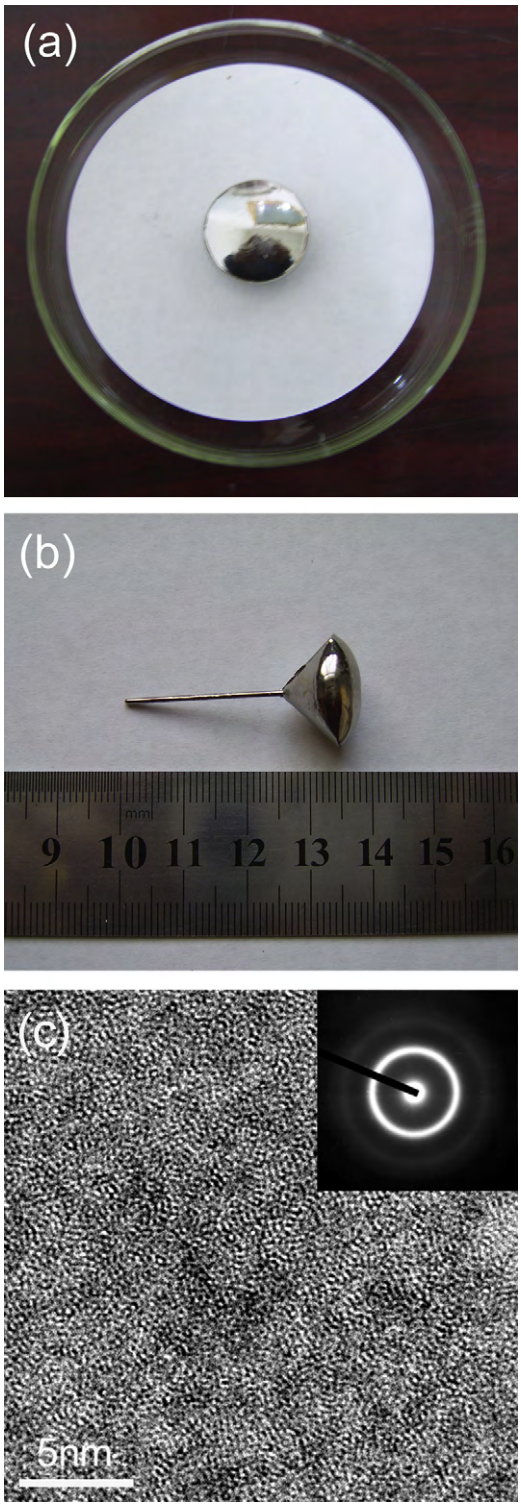

Fig. 1. Image of Ti–Cu–Zr–Ni–Sn alloy (a) ingot, (b) suction-cast rod, and (c) the morphologies of HRTEM for $(Ti_{0.45}Cu_{0.378}Zr_{0.10}Ni_{0.072})_{98}Sn_2$ glassy alloy in ϕ 2 mm as-cast rod.

3. Results

Fig. 2(a) shows the XRD patterns of the as-prepared $(Ti_{0.45}Cu_{0.378}Zr_{0.10}Ni_{0.072})_{100-x}Sn_x$ (x = 0, 2, 4, 6 and 8) alloys with a diameter of 1 mm. Except for one broad diffraction peak, no distinctive sharp diffraction peak of crystallization is observed in the XRD spectra of $(Ti_{0.45}Cu_{0.378}Zr_{0.10}Ni_{0.072})_{100-x}Sn_x$ alloy as

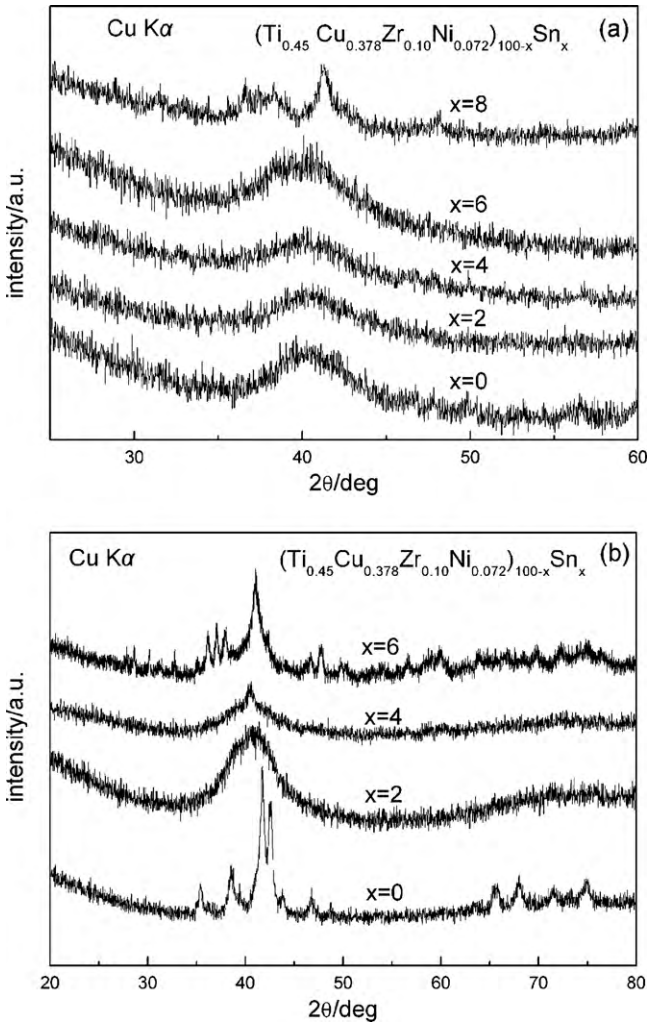

Fig. 2. (a) XRD patterns of alloys of $(Ti_{0.45}Cu_{0.378}Zr_{0.10}Ni_{0.072})_{100-x}Sn_x$ (x = 0–8) with a diameter 1 mm and (b) XRD patterns of alloys of $(Ti_{0.45}Cu_{0.378}Zr_{0.10}Ni_{0.072})_{100-x}Sn_x$ (x = 0–6) with a diameter 2 mm.

x is 0, 2, 4 and 6, respectively. This indicates that these alloys are composed of a glassy phase. However, for alloy of x = 8, several obvious sharp diffraction peaks are detected, which illustrates that this alloy is not of full amorphous state. For alloys with x = 0, 2, 4 and 6, we further studied and compared their glass-forming ability. Fig. 2(b) shows the X-ray diffraction (XRD) patterns of the as-prepared $(Ti_{0.45}Cu_{0.378}Zr_{0.10}Ni_{0.072})_{100-x}Sn_x$ (x = 0, 2, 4 and 6) alloys with a diameter of 2 mm. It is obvious that sharp diffraction peaks of crystallization could be observed in the XRD spectra for all alloys except for alloy with x = 2. Apparently, with x = 2, the $(Ti_{0.45}Cu_{0.378}Zr_{0.10}Ni_{0.072})_{98}Sn_2$ alloy possesses the best GFA among present Ti–Zr–Cu–Ni–Sn alloy system, and the critical diameter for glass-forming ability is 2 mm. Its microstructure has also been confirmed by HRTEM image (Fig. 1(c)). The dark-field transmission electron micrograph is featureless, and the selected electron diffraction pattern exhibits typical halo rings, which is inherent for amorphous phase.

Fig. 3 and Table 1 shows DSC traces of $(Ti_{0.45}Cu_{0.378}Zr_{0.10}Ni_{0.072})_{100-x}Sn_x$ (x = 0, 2, 4 and 6) glassy alloys and the thermal parameters derived from the DSC curves respectively. The glass transition temperature T_g and the initial crystallization temperature T_x increase with increasing Sn content. For example, T_x increases from 680 K for alloy of x = 0 ($Ti_{45}Cu_{37.8}Zr_{10}Ni_{7.2}$) to 739 K for alloy of x = 6

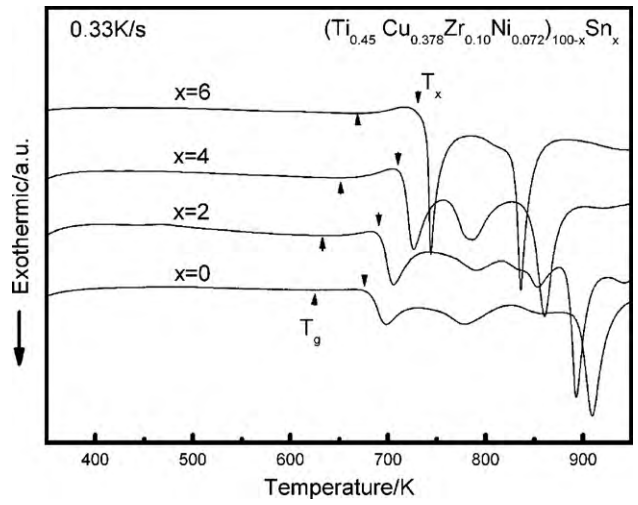

Fig. 3. Traces of DSC of alloys $(Ti_{0.45}Cu_{0.378}Zr_{0.10}Ni_{0.072})_{100-x}Sn_x$ (x = 0–6) measured at 0.33 K s^{-1}.

Table 1
Thermal parameters of $(Ti_{0.45}Cu_{0.378}Zr_{0.10}Ni_{0.072})_{100-x}Sn_x$ alloys.

x	T_g (K)	T_x (K)	ΔT_x (K)	T_m (K)	T_l (K)	T_{rg}	γ
0	641	680	39	1005	1167	0.549	0.376
2	650	692	42	1016	1167	0.557	0.381
4	666	715	49	1017	1156	0.570	0.392
6	683	739	56	1116	1169	0.584	0.399

$(Ti_{0.45}Cu_{0.378}Zr_{0.10}Ni_{0.072})_{94}Sn_6$ (see Table 1). The supercooled liquid region ΔT_x ($\Delta T_x = T_x - T_g$) of the glassy alloys also increases from 39 K for x = 0 alloy to 56 K for x = 6 alloy. The reduced glass transition temperature T_{rg} and the parameter γ (defined as $T_x/(T_g + T_l)$) increased from 0.549 and 0.376 for x = 0 alloy to 0.584 and 0.399 for x = 6 alloy, respectively.

Fig. 4 shows the compressive stress–strain curves of $(Ti_{0.45}Cu_{0.378}Zr_{0.10}Ni_{0.072})_{100-x}Sn_x$ (x = 0, 2, 4 and 6) glassy alloys. It is seen that no obvious plasticity could be observed for alloys with x = 0 and x = 6, and a plastic strain of about 7.6% and 1% could be observed for alloy with x = 2 and x = 4, respectively. The fracture strength for these four alloys is 2360, 2650, 2500, and 1820 MPa, respectively.

Fig. 5(a)–(c) shows the fractographic morphologies of $(Ti_{0.45}Cu_{0.378}Zr_{0.10}Ni_{0.072})_{98}Sn_2$ and $Ti_{45}Cu_{37.8}Zr_{10}Ni_{7.2}$ BMG samples, and (d), (e) and (f) shows the side view images of the

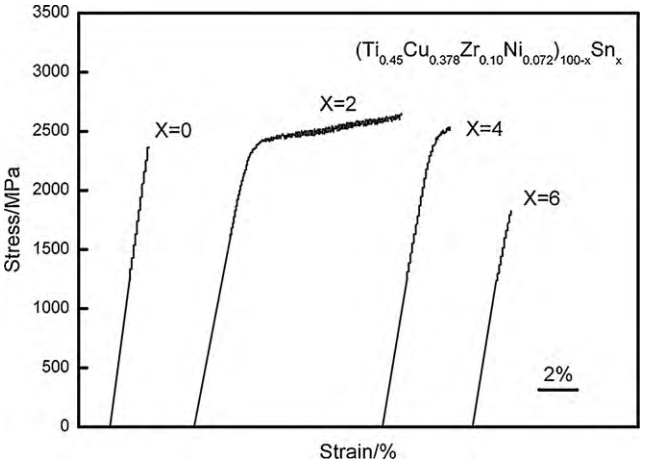

Fig. 4. The compressive stress–strain curves of $(Ti_{0.45}Cu_{0.378}Zr_{0.10}Ni_{0.072})_{100-x}Sn_x$ (x = 0–6) bulk glassy alloy (samples size: ϕ 1 mm × 2 mm).

Table 2
The atomic sizes and mixing heats with each others.

	ΔH^{mix} (kJ mol^{-1})					Radius (Å)
	Sn	Ti	Cu	Zr	Ni	
Sn		−21	7	−43	−4	1.51
Ti	−21		−15	0	−35	1.47
Cu	7	−15		−23	4	1.28
Zr	−43	0	−23		−49	1.62
Ni	−4	−35	4	−49		1.25

deformed $(Ti_{0.45}Cu_{0.378}Zr_{0.10}Ni_{0.072})_{98}Sn_2$ and $Ti_{45}Cu_{37.8}Zr_{10}Ni_{7.2}$ BMG samples. The river-like pattern (see Fig. 5(b)) and vein-like pattern (see Fig. 5(c)), which are typical fracture morphologies of glassy alloys [1,2,18–21], are observed. Some melt drops are observed on the fracture surface (Fig. 5(b)). Many parallel shear bands are observed in Fig. 5(d). Fig. 5(e) is an enlarged image of the area indicated by the white arrow in Fig. 5(d), clearly showing the primary shear bands and a lot of secondary shear bands, some of them are originated from the primary shear bands and of an approximate 45° with the primary shear band. Different from the morphology observed in Fig. 5(d) and (e), almost no shear band has been observed in the area far away from the fracture surface of the $Ti_{45}Cu_{37.8}Zr_{10}Ni_{7.2}$ BMG sample. Even in the area near the fracture surface, only few shear bands are observed (Fig. 5(f)) and no secondary shear band has been clearly observed. In addition, protruded melts along the primary shear bands are observed, indicating the existences of overheating resulted from shear localization. It is known that the more the shear bands generate, the larger the plasticity of BMGs is [22–25]. That is the plasticity of BMGs is closely related to the number of activated shear bands [26,27]. Fig. 5 agrees with the results shown in Fig. 4.

4. Discussions

As show in Table 1, the value of the supercooled liquid region ΔT_x of the $Ti_{45}Cu_{37.8}Zr_{10}Ni_{7.2}$ alloy is greatly increased with the addition of Sn. The ΔT_x value reflects mainly thermal stability of the supercooled liquid and is also associated with the glass-forming ability of metallic glasses [28]. It suggests that the GFA of the alloy may be enhanced by suitable addition of element Sn [29,30]. In order to understand the reason, the atomic size and mixing heat among the constituents of the alloys (see Table 2) have been examined [31,32]. It shows that the radius of Sn atom is larger than that of Cu, Ni and Ti but smaller than that of Zr. And the absolute value of mixing heats between Sn and Zr is relatively large. It implies that the large atoms Sn and Zr have the tendency to get together, which would result in increasing the difficulty of inter-atomic diffusion. Then the stability of the undercooled melt and the supercooled liquid would be enhanced. This may be the reason why ΔT_x and GFA of the alloy are increased. But why the alloy with the addition of 2 at.% Sn exhibits better GFA is still unclear.

Fig. 4 shows that with the addition of 2 at.% Sn in the alloy the plastic strain of the alloy $Ti_{45}Cu_{37.8}Zr_{10}Ni_{7.2}$ is enhanced from almost zero to 7.6% strain. And SEM images also show that abundant of shear bands, especially a lot of secondary ones, have been activated during deformation. It suggests that the shear localization in the initial deformation stage has been hindered and the multiplication of the shear bands have been promoted by the addition of Sn element. But no nano-crystalline precipitates or chemical structural inhomogeneity, which are reported to benefit the enhancement of BMGs' plasticity, have been clearly observed. The mechanism of Sn addition affecting the plasticity of the Ti–Zr–Cu–Ni alloy is not clear. It is worth to study further.

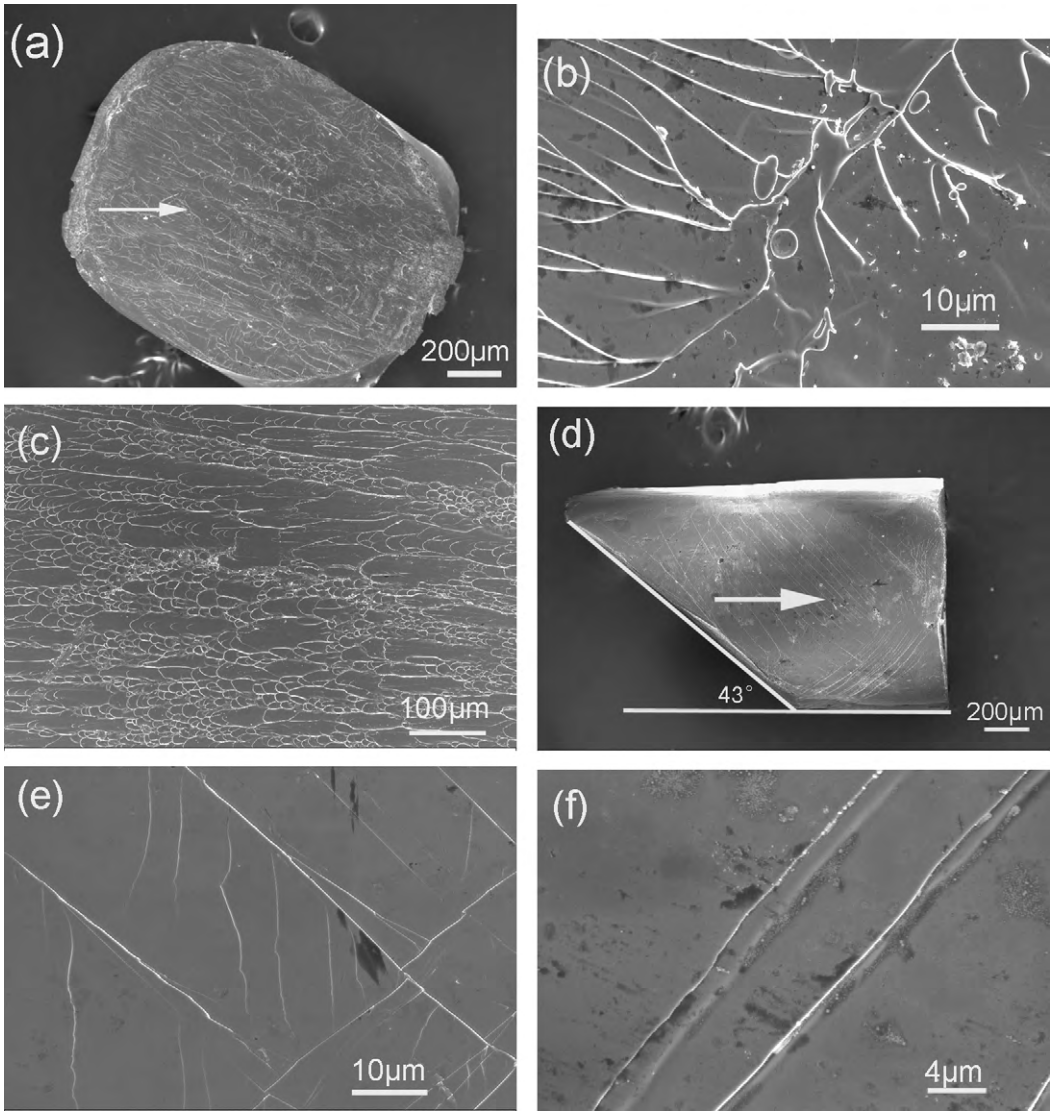

Fig. 5. (a) and (b) are low and high magnification SEM images of the fractographic morphology of $(Ti_{0.45}Cu_{0.378}Zr_{0.10}Ni_{0.072})_{98}Sn_2$ alloy, respectively. (c) The fractographic image of $Ti_{45}Cu_{37.8}Zr_{10}Ni_{7.2}$ alloy. (d) SEM side view image of a deformed $(Ti_{0.45}Cu_{0.378}Zr_{0.10}Ni_{0.072})_{98}Sn_2$ samples. (e) High magnification image of the area indicated by white arrow in (d), showing a lot of primary and secondary shear bands. (f) SEM side view image of the $Ti_{45}Cu_{37.8}Zr_{10}Ni_{7.2}$ glassy sample taken near the fracture surface.

5. Conclusions

(1) The glassy alloys of $(Ti_{0.45}Cu_{0.378}Zr_{0.10}Ni_{0.072})_{100-x}Sn_x$ ($x = 0$, 2, 4, and 6) are prepared with copper-mold casting method. The addition of Sn in the Ti–Cu–Zr–Ni alloy without containing Pd or Be is efficient to enhance the glass-forming ability of the Ti–Cu–Zr–Ni alloy and to increase the supercooled liquid range. The optimized addition of Sn is about 2% in atomic percent.

(2) The as-prepared $(Ti_{0.45}Cu_{0.378}Zr_{0.10}Ni_{0.072})_{98}Sn_2$ bulk glassy alloy exhibits high strength and large plasticity at room temperature. Its yield strength σ_y, fracture strength σ_f, and compressive plastic strain ε_p are 2260, 2650 MPa and 7.6%, respectively.

Acknowledgements

This work is supported by National Basic Research Program of China (Grant No. 2007CB613905) and National Natural Science Foundation of China (Grant Nos. 50671050 and 50971073). The authors acknowledge the supports from the National Center of Nano-Science and Nano-Technology of China, the Analysis Center of Tsinghua University.

References

[1] W.H. Wang, C. Dong, C.H. Shek, Mater. Sci. Eng. R 44 (2004) 45.
[2] A. Inoue, Acta Mater. 48 (2000) 279.
[3] Y.C. Kim, W.T. Kim, D.H. Kim, Mater. Sci. Eng. A 375–377 (2004) 127.
[4] T. Zhang, A. Inoue, T. Masumo, Mater. Sci. Eng. A 181–182 (1994) 1423.
[5] X.H. Lin, W.L. Johnson, J. Appl. Phys. 78 (1995) 6514.
[6] T. Zhang, A. Inoue, Mater. Trans. JIM 10 (1998) 1001.
[7] D.V. Louzguine, A. Inoue, Scripta Mater. 43 (2000) 371.
[8] T. Zhang, A. Inoue, Mater. Sci. Eng. A 304–306 (2001) 771.
[9] G. Duan, A. Wiest, M.L. Lind, A. Kahl, W.L. Johnson, Scripta Mater. 58 (2008) 465.
[10] S.L. Zhu, X.M. Wang, F.X. Qin, A. Inoue, Mater. Sci. Eng. A 459 (2007) 233.
[11] S.L. Zhu, X.M. Wang, F.X. Qin, A. Inoue, Intermetallics 16 (2008) 1031.
[12] Y.L. Wang, J. Xu, Metall. Mater. Trans. 39A (2008) 2990.
[13] X.F. Wu, Z.Y. Suo, Y. Si, L.K. Meng, K.Q. Qiu, J. Alloys Compd. 452 (2008) 268.
[14] Y.L. Wang, E.A. Ma, J. Xu, Phil. Mag. Lett. 88 (2008) 319.
[15] N. Nishiyama, K. Amiya, A. Inoue, J. Non-Cryst. Solids 353 (2007) 3615.
[16] O. Jeong-Jung, D.V. Louzguine-Luzgin, A. Inoue, Appl. Phys. Lett. 91 (2007) 053106.
[17] Y.C. Wang, N. Chen, K.F. Yao, Chin. Phys. Lett. 24 (2007) 1653.
[18] S.B. Qiu, K.F. Yao, Appl. Surf. Sci. 2554 (2008) 3454.
[19] S.B. Qiu, K.F. Yao, P. Gong, Sci. China Sers. G-Phys. Mech. Astron. 53 (2010) 1.

[20] Y.J. Huang, J. Shen, J.F. Sun, Appl. Phys. Lett. 90 (2007) 081919.
[21] W.L. Johnson, J. Lu, M.D. Demetriou, Intermetallics 10 (2002) 1039.
[22] G. He, J. Eckert, Q.L. Dai, Biomaterials 24 (2003) 5115.
[23] K.F. Yao, F. Ruan, Y.Q. Yang, N. Chen, Appl. Phys. Lett. 88 (2006) 122106.
[24] Y.C. Kim, H.J. Chang, D.H. Kim, J. Phys. Condens. Mater. 19 (2007) 196104.
[25] K.F. Yao, C.Q. Zhang, Appl. Phys. Lett. 90 (2007) 061901.
[26] M.X. Xia, H.X. Zheng, J. Liu, C.L. Ma, J.G. Li, J. Non-Cryst. Solids 351 (2005) 3747.
[27] Y.J. Huang, J. Shen, J.F. Sun, Z.F. Zhang, Mater. Sci. Eng. A 498 (2008) 203.
[28] L.C. Zhang, H.-B. Lu, M. Christine, J. Eckert, Appl. Phys. Lett. 91 (2007) 051906.
[29] W.Z. Liang, J. Shen, J.F. Sun, L.Z. Wu, P.K. Liaw, Mater. Sci. Eng. A 497 (2008) 378.
[30] X.L. Ji, Y. Pan, Mater. Sci. Eng. A 485 (2008) 154.
[31] A. Takeuchi, A. Inoue, Mater. Trans. 46 (2005) 2817.
[32] B.X. Liu, W.S. Lai, Q. Zhang, Mater. Sci. Eng. A 244 (2000) 1.